

Improving Liver Disease Diagnosis with SNNDeep: A Custom Spiking Neural Network Using Diverse Learning Algorithms

Zofia Rudnicka

Janusz Szczepanski

Agnieszka Pregowska*

Institute of Fundamental Technological Research,
Polish Academy of Sciences,
Pawinskiego 5B, 02-106 Warsaw, Poland

Abstract

Purpose: Spiking neural networks (SNNs) have recently gained attention as energy-efficient, biologically plausible alternatives to conventional deep learning models. Their application in high-stakes biomedical imaging remains almost entirely unexplored. **Methods:** This study introduces SNNDeep, the first tailored SNN specifically optimized for binary classification of liver health status from computed tomography (CT) features. To ensure clinical relevance and broad generalizability, the model was developed and evaluated using the Task03_Liver dataset from the Medical Segmentation Decathlon (MSD), a standardized benchmark widely used for assessing performance across diverse medical imaging tasks. We benchmark three fundamentally different learning algorithms, namely Surrogate Gradient Learning, the Tempotron rule, and Bio-Inspired Active Learning across three architectural variants: a fully customized low-level model built from scratch, and two implementations using leading SNN frameworks, i.e., `snnTorch` and `SpikingJelly`. Hyperparameter optimization was performed using `Optuna`. **Results:** Our results demonstrate that the custom-built SNNDeep consistently outperforms framework-based implementations, achieving a maximum validation accuracy of 98.35%, superior adaptability across learning rules, and significantly reduced training overhead. **Conclusion:** This study provides the first empirical evidence that low-level, highly tunable SNNs can surpass standard frameworks in medical imaging, especially in data-limited, temporally constrained diagnostic settings, thereby opening a new pathway for neuro-inspired AI in precision medicine.

Keywords: Spiking Neural Networks (SNN), Liver Disease Classification, Medical Image Analysis, Bio-Inspired Machine Learning

1 Introduction

Liver diseases remain among the leading causes of morbidity and mortality worldwide, with hepatocellular carcinoma, cirrhosis, and non-alcoholic fatty liver disease accounting for a substantial share of the global healthcare burden [1]. Thus, early and efficient diagnosis of liver pathology is crucial to improve therapeutic outcomes, provide timely intervention, and reduce disease progression [2]. Recently, medical imaging, particularly computed tomography (CT), has played a key role in the noninvasive assessment of liver structure and function [3]. However, manual interpretation of CT scans is labor intensive, subject to interobserver variability, and constrained by the limited availability of expert radiologists [4]. These limitations have accelerated the development of machine learning-based automated diagnostic systems to support clinicians in image-based decision making.

Despite the remarkable success of convolutional neural networks in liver lesion detection and classification, their substantial computational requirements and restricted temporal modeling capabilities underscore the opportunity for bio-inspired approaches [5, 6]. Spiking Neural Networks (SNNs), with their event-driven computation and closer resemblance to biological neural coding, offer a promising, however, underexplored alternative for liver CT classification [7–9].

Several recent studies have demonstrated the strong potential of spiking neural networks in medical image classification, although applications have largely been limited to organs such as the lungs, brain,

*Corresponding author: aprego@ippt.pan.pl

skin, and breast [10]. For example, a Tempotron-based SNN augmented with spike-timing-dependent plasticity (STDP) achieved 98.32% accuracy in tuberculosis detection from chest X-ray datasets such as KIT, Shenzhen, and Montgomery [11]. This approach leveraged both the temporal precision of spike-based computation and the biological interpretability of synaptic plasticity.

In dermatology, SNNs trained with surrogate gradient learning have been applied to dermoscopy images for melanoma detection, attaining accuracy levels near 89.60% [12]. Similarly, a multi-spike architecture with temporal feedback mechanisms has been used for breast cancer diagnosis, reporting performance up to 98.00% [13].

Beyond organ specific tasks, some efforts have aimed to build generalizable SNN frameworks. The SNMID system, for instance, combined wavelet and histogram based features to classify diverse pathologies, including malaria, breast cancer, and skin lesions, with competitive results, e.g., 91.20% accuracy for malaria. However, its reliance on handcrafted features and the absence of optimization for temporal spike learning limited its scalability [14]. While these studies confirm the adaptability of SNNs to diverse diagnostic tasks, their potential for liver CT classification remains essentially untapped, representing a clear opportunity for advancement, remains essentially untapped, representing a clear opportunity for advancement [15].

This study addresses the identified research gap by presenting the first comprehensive benchmark of spiking neural networks for binary classification of liver health status from CT imaging. The central contribution is SNNDeep, a three-layer, fully custom built SNN designed specifically for hepatic image analysis. Unlike most SNN implementations that rely on fixed components from open source frameworks, SNNDeep is constructed entirely from the ground up, enabling fine-grained control over neuron dynamics, spike generation, and synaptic updates. This low level design facilitates seamless integration of diverse biologically inspired learning rules without architectural compromises.

To systematically evaluate learning strategy effects, we benchmark three biologically grounded training methods: Surrogate Gradient Descent, the Tempotron rule, and Bio Inspired Active Learning (BAL) [16], across three architectural variants: (1) the handcrafted SNNDeep model, (2) a `snnTorch` implementation, and (3) a SpikingJelly implementation. While these frameworks are widely used in the SNN community, their abstraction layers can limit configurability and performance in specialized biomedical tasks. All models were trained and evaluated on the from the Medical Segmentation Decathlon database, with hyperparameters optimized using Optuna.

2 Materials and Methods

2.1 Neuron model

The Leaky Integrate-and-Fire (LIF) neuron forms the computational core of the proposed SNNDeep architecture. LIF is a widely adopted abstraction of biological spiking neurons, balancing biophysical plausibility with computational efficiency [17]. The membrane potential evolves as

$$\tau_m \frac{dV_m(t)}{dt} = -V_m(t) + R_m I(t), \quad (1)$$

where τ_m is the membrane time constant, R_m the membrane resistance, and $I(t)$ the synaptic input. When $V_m(t)$ exceeds V_{th} , the neuron emits a spike and resets to V_{reset} .

Unlike previous biomedical SNN implementations that employ fixed LIF parameters, SNNDeep optimizes neuron dynamics (time constants, thresholds, and reset mechanisms) for liver CT data and across three learning paradigms (Surrogate Gradient, Tempotron, BAL). This targeted tuning enhances both classification accuracy and temporal adaptability, demonstrating the benefit of customized LIF behavior in data-limited clinical applications.

2.2 Network architecture

The proposed model, SNNDeep, is a three-layer spiking neural network tailored for binary classification of liver health status (healthy *versus* diseased) from CT-derived features. The architecture consists of an input layer for temporally encoded spike trains, two hidden layers of LIF neurons for hierarchical temporal feature extraction, and a fully connected output layer producing classification logits, as shown in Figure 1. A distinctive contribution of this study is the implementation of SNNDeep in three computationally distinct variants: a custom low-level build and two framework-based models using `snnTorch` and SpikingJelly. This enables a rare cross-framework benchmark of different learning algorithms.

All models were subjected to systematic hyperparameter optimization using Optuna, targeting membrane time constants, thresholds, temporal encoding schemes, and neuron population sizes. The optimal configurations, selected through a validation accuracy, were subsequently evaluated on the Task03_Liver dataset. This design provides a fair and reproducible basis for comparing custom and framework-based SNNs, highlighting the performance benefits of low-level, highly tunable architectures in liver CT classification.

To ensure reproducibility, all architectural parameters were fully specified and standardized across implementations. In the custom SNNDeep model, both hidden layers consisted of LIF neurons with membrane time constant τ_m optimized in $[1.1, 3.0]$, spike threshold V_{th} tuned in $[0.2, 0.8]$, and synaptic bias b in $[0.0, 0.05]$. The first and second hidden layers contained $[64, 128]$ and $[32, 64]$ neurons respectively, optimized using Optuna’s Bayesian search. Temporal encoding was implemented using both Poisson-based and rate-based schemes, with spike trains generated from a homogeneous Poisson process (mean rate λ optimized) over 5–20 simulation steps per input. All implementations were developed in PyTorch 2.2.2 with CUDA 12.1; framework variants used snnTorch 0.9.0 and SpikingJelly 0.0.0.13, ensuring environment reproducibility.

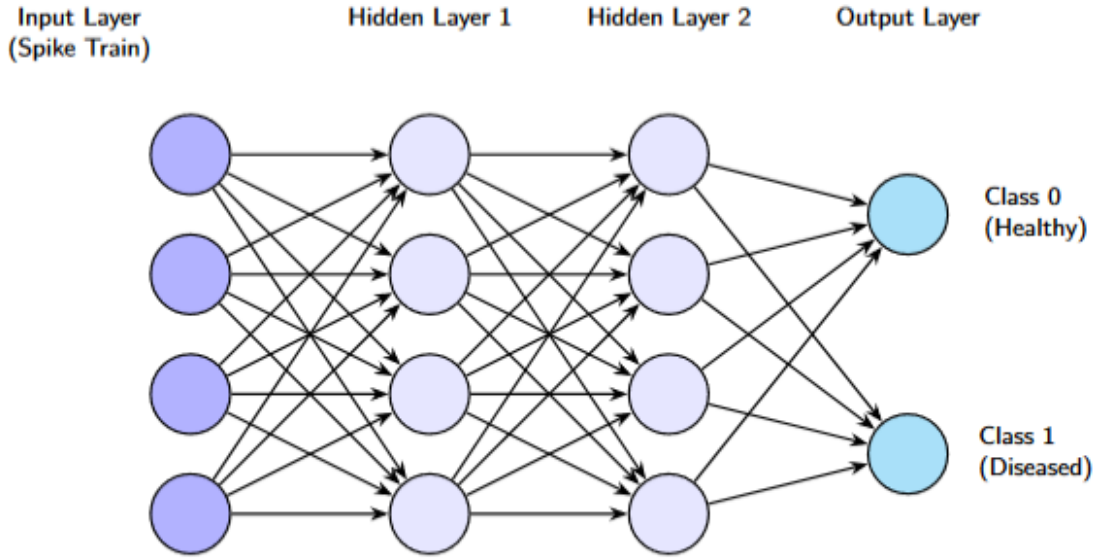


Figure 1: SNNDeep architecture.

2.3 Learning algorithms

We evaluate three supervised learning rules in SNNDeep: Tempotron, Bio-Inspired Active Learning, and Surrogate Gradient Learning. All methods are implemented with LIF neurons and share identical topology, allowing a fair comparison.

2.3.1 Tempotron Learning Rule

The Tempotron [18] emphasizes precise spike timing for classification. The membrane potential $v(t)$ of an LIF neuron is computed as

$$v(t) = \sum_i \omega_i \sum_{t_i} K(t - t_i) + V_{\text{rest}}, \quad (2)$$

where ω_i denotes the synaptic weight of the i -th input, t_i are the presynaptic spike times, V_{rest} is the resting membrane potential, and $K(t - t_i)$ is the postsynaptic potential (PSP) kernel. The kernel is given by

$$K(t - t_i) = V_0 \left(e^{-\frac{t-t_i}{\tau_m}} - e^{-\frac{t-t_i}{\tau_s}} \right), \quad (3)$$

where V_0 is a normalization factor ensuring a peak of 1, τ_m is the membrane time constant, and τ_s is the synaptic time constant. Weight updates are based on the time t_{\max} at which $v(t)$ reaches its maximum:

$$\Delta\omega_i = \lambda \sum_{t_i < t_{\max}} K(t_{\max} - t_i), \quad (4)$$

where λ is the learning rate, positive for potentiation (P^+) and negative for depression (P^-).

2.3.2 Bio-Inspired Active Learning

BAL combines spike-timing plasticity with active data selection. Each weight w_{ij} is associated with an uncertainty $U(w_{ij})$ [19]. The update rule prioritizes inputs expected to reduce synaptic uncertainty:

$$\Delta w_{ij} \propto U(w_{ij}) \cdot \mathbb{E}_{x \in \mathcal{D}} [I(S_{\text{post}}; S_{\text{pre}} \mid x)], \quad (5)$$

where \mathcal{D} is the set of unlabeled input patterns, S_{pre} and S_{post} denote pre- and postsynaptic spike trains, and $I(S_{\text{post}}; S_{\text{pre}})$ is their mutual information. The latter is defined as

$$I(S_{\text{post}}; S_{\text{pre}}) = H(S_{\text{post}}) - H(S_{\text{post}} \mid S_{\text{pre}}), \quad (6)$$

where $H(\cdot)$ represents Shannon entropy.

2.3.3 Surrogate Gradient Learning

SGL addresses the non-differentiability of spike generation by replacing the derivative of the Heaviside function with a smooth surrogate [20]:

$$\sigma'(V) = \alpha \cdot \exp(-\alpha(V - 1)^2), \quad (7)$$

where α controls the smoothness and V is the membrane potential. The error signal is computed as

$$\delta = \eta \cdot (y - \hat{y}) \cdot \sigma'(V), \quad (8)$$

where η is the learning rate, y the target output, and \hat{y} the predicted output. Weights are updated layer-wise, for example:

$$\Delta W_{h2, \text{out}} = h_2^\top \delta, \quad \Delta W_{h1, h2} = h_1^\top (W_{h2, \text{out}} \cdot \delta), \quad (9)$$

where h_1 and h_2 are the spike activations of the hidden layers.

2.4 Input datasets

This study uses the Task03_Liver dataset from the Medical Segmentation Decathlon (MSD) [21], a standardized benchmark for evaluating generalization across diverse medical image tasks. Task03_Liver contains abdominal computed tomography volumes focusing on liver parenchyma and hepatic lesions. The data are provided as three-dimensional (3D) scans in NIfTI format (`.nii.gz`), accompanied by ground-truth segmentation masks G_i manually annotated by expert radiologists for each scan V_i . For this work, segmentation labels are reformulated into binary class labels based on the presence of pathology:

$$y_i = \begin{cases} 0 & \text{if healthy liver (no lesion)} \\ 1 & \text{if diseased liver (lesion present)} \end{cases} \quad \text{for } i = 1, 2, \dots, N$$

From each pair (V_i, G_i) , a diagnostic feature vector $F_i \in \mathbb{R}^d$ is extracted, summarizing morphological and intensity-based properties of liver tissue. These vectors are then temporally encoded into spike trains and used as inputs to the spiking neural network. By abstracting from voxel-wise segmentation, this setup allows a controlled binary classification task and enables evaluation of spiking networks' ability to infer liver health status from temporal feature representations.

Table 1: Validation accuracy and training time for each SNNDeep implementation and learning rule. Best accuracy per column is highlighted in bold.

Model	Learning Rule	Accuracy (%)	Training Time (s)
Custom SNNDeep	Surrogate Gradient	98.35	108 870
	Tempotron	95.19	58 878
	BAL	97.19	64 321
snnTorch	Surrogate Gradient	95.19	75 834
	Tempotron	95.19	45 140
	BAL	95.19	67 513
SpikingJelly	Surrogate Gradient	95.19	301 642
	Tempotron	95.19	57 058
	BAL	95.19	114 669

3 Results

We evaluated three implementations of the proposed SNNDeep model (1) a fully custom build, (2) a snnTorch-based variant, and (3) a SpikingJelly-based variant. Each combined with three learning algorithms: Surrogate Gradient, Tempotron, and Bio-Inspired Active Learning. All models were trained and validated under identical conditions (i.e., dataset splits, encoding, hyperparameter tuning with Optuna) to ensure a fair comparison. Validation accuracy and total training time are summarized in Table 1. All computations were provided on Intel(R) Core(TM) i7-14700F, 2.10 GHz.

The custom implementation consistently outperformed framework-based variants. Using SG learning, it achieved the highest validation accuracy of 98.35% with a training time of 108,870 seconds. BAL also yielded strong results (97.19%) with moderate training cost, while Tempotron achieved 95.19% accuracy with the shortest training time (58,878 seconds). In comparison, snnTorch and SpikingJelly stabilized at 95.19% accuracy across all learning rules. Although SpikingJelly supports fine-grained neuronal simulation, its surrogate gradient training required more than 301,000 seconds, indicating limited computational efficiency for large-scale training, see Figure 2.

The observed performance differences are primarily attributable to the architectural transparency of the custom implementation. By providing explicit control over spike encoding, membrane potential decay, threshold mechanisms, and synaptic plasticity, the handcrafted design allowed precise alignment between network dynamics and the specific requirements of each learning rule. In contrast, the higher level abstractions imposed by framework based implementations constrained this flexibility, limiting adaptability, particularly for non gradient learning strategies such as Tempotron and BAL.

4 Discussion

Our results demonstrate that all evaluated SNNDeep configurations, including the custom-built implementation as well as the snnTorch and SpikingJelly variants, outperformed previously reported methods for liver disease classification, both in predictive accuracy and methodological robustness. This advantage was consistent across all architectural and algorithmic combinations.

For example, [22] reported 85.60% accuracy for a contrastive fusion deep neural network applied to non-invasive liver fibrosis staging from ultrasound images. While this represents a meaningful result in the ultrasound-based diagnostic domain, it remains well below the accuracy of all our CT-based models, each of which exceeded 95.00% regardless of the learning rule applied. Notably, our custom SNNDeep model trained with surrogate gradient learning achieved a top validation accuracy of 98.35%, extending the performance range for liver disease classification in a CT context.

While part of this advantage over ultrasound models may be due to the higher spatial resolution and reduced operator-dependence of CT, the consistent performance of SNNDeep across all learning paradigms indicates that architectural and algorithmic factors also play a key role. The network’s temporal encoding, biologically inspired learning mechanisms, and fine-grained hyperparameter tuning suggest that the improvements are not modality-specific but stem from the model’s ability to exploit temporal structure

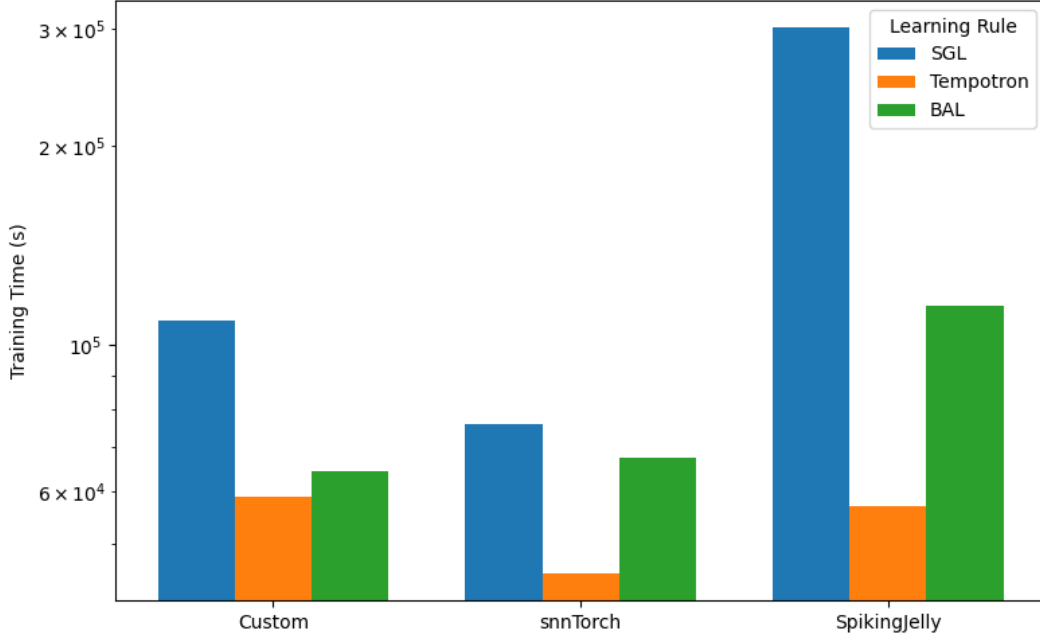


Figure 2: Training time by framework and learning algorithm.

and spike dynamics.

The performance gap becomes even more pronounced when compared to the metaheuristic-trained SNN proposed by [23], evaluated on the UCI Liver Disorders dataset, which achieved 68.70% accuracy. Despite using computationally intensive optimization, their model did not approach the performance of even the least effective configuration in our experiments. In our study, the lowest recorded accuracy, obtained by the Tempotron-trained snnTorch variant, was 95.19%, indicating a margin of over 26 percentage points compared to the metaheuristic SNN.

Instead of evidential networks, recently [24] introduced the Dynamic Recurrent Inference Machine (DRIM) for reconstructing sparsely sampled 4D liver MRI by exploiting correlations between respiratory states. Applied in an MR-guided radiotherapy protocol for liver lesions, DRIM improved the SSIM score from approximately 0.89 (RIM baseline) to 0.95, enabling 2.7-fold faster acquisition with clinically acceptable sharpness at acceleration factors up to 10 times.

Beyond SNN-based methods, conventional convolutional neural networks have also been extensively applied to liver disease classification and staging. The study [27] developed a deep CNN for staging liver fibrosis using contrast-enhanced CT, achieving 79.40% accuracy with AUCs of 0.95-0.97 for different fibrosis thresholds. Other paper, [26] applied a deep CNN to gadoxetic acid-enhanced hepatobiliary-phase MRI, obtaining AUCs of approximately 0.84–0.85 for advanced fibrosis detection. More recently, [28] used a deep CNN with Grad-CAM explainability to stage liver fibrosis on MRI, reporting AUC values of 0.88-0.92. While these CNN-based models demonstrate clinical feasibility and good performance, they typically plateau below the 90-94.00% range and operate primarily in 2D or 2.5D, limiting their ability to capture temporal dynamics. Furthermore, dense convolutional operations increase computational cost, making them less adaptable to event-driven or low-power neuromorphic deployment.

In comparison, SNNDeep consistently exceeded 95.00% accuracy across all tested learning paradigms, with the custom surrogate-gradient-trained model achieving 98.35%. This suggests that the superior performance is driven not only by the CT modality but also by the deliberate integration of biologically informed learning rules, temporal coding, and architecture-level optimization.

From a translational perspective, the proposed framework aligns with practical considerations for deployment in clinical environments. Its compact three-layer design and compatibility with event-driven computation make it suitable for energy-efficient neuromorphic hardware (e.g., Intel Loihi, SpiNNaker) or edge-computing PACS integration. Such deployment could facilitate real-time decision support in radiology workflows, particularly in settings with limited access to subspecialist expertise. Prospective validation on independent, multicenter cohorts will be a critical step toward clinical translation, ensuring

robustness across different scanner protocols, institutions, and patient populations.

5 Limitations of the study

This study is limited by its focus on binary liver health classification using a dataset (Task03_Liver) and needs further external clinical validation. While this controlled setup was appropriate for benchmarking SNN architectures, future work should address multiclass scenarios, evaluate generalizability across institutions, and integrate additional learning rules, e.g., STDP variants, reinforcement-driven plasticity. Moreover, deployment on neuromorphic hardware could further improve latency and energy efficiency, enhancing the framework’s translational potential.

Moreover, extending SNNDeep to multimodal datasets, i.e., combining CT with MRI and ultrasound, could further strengthen its clinical applicability and provide a more comprehensive evaluation of its performance relative to other modalities. Finally, deployment on neuromorphic hardware could improve latency and energy efficiency, enhancing the framework’s translational potential in real-time clinical workflows.

6 Conclusion

This study presented a comprehensive benchmark of spiking neural networks for liver disease classification, comparing three learning algorithms, namely Surrogate Gradient, Tempotron, and Bio-Inspired Active Learning across custom and framework, based implementations of the proposed SNNDeep architecture. The custom low-level model consistently outperformed `snnTorch` and `SpikingJelly` variants, achieving up to 98.35% validation accuracy and demonstrating superior adaptability across learning rules.

These results highlight the benefits of direct control over spike dynamics, synaptic integration, and learning mechanisms, confirming that handcrafted SNNs can exceed the performance of general-purpose frameworks in computationally constrained and clinically focused tasks. The findings provide a foundation for extending SNNDeep to multiclass problems, integrating additional biologically inspired rules, and evaluating real-world deployment in multicenter clinical datasets.

Declarations

- Funding: not applicable
- Conflict of interest/Competing interests: the authors declare that they have no known competing financial interests or personal relationships that could have appeared to influence the work reported in this paper.
- Ethics approval and consent to participate: the authors affirm that this work adheres to the highest ethical standards of scientific publication, in accordance with COPE guidelines.
- Consent for publication: not applicable
- Data availability: This work uses the Task03_Liver dataset from the Medical Segmentation Decathlon (MSD) [21].
- Materials availability: not applicable
- Code availability: not applicable
- Author contribution: all authors contributed to the conception and design of the study. All authors performed material preparation, data collection, and analysis. The first draft of the manuscript was written by all authors who commented on previous versions of the manuscript. All authors read and approved the final manuscript.

[1] Guo Z, Wu D, Mao R et al (2025) Global burden of MAFLD, MAFLD related cirrhosis and MASH related liver cancer from 1990 to 2021. *Scientific Reports* 15:7083. <https://doi.org/10.1038/s41598-025-91312-5>

[2] Pozowski P, Bilski M, Bedryło M, Sitny P, Zaleska-Dorobisz U (2025) Modern ultrasound techniques for diagnosing liver steatosis and fibrosis: A systematic review with a focus on biopsy comparison. *World Journal of Hepatology* 17(2):100033. <https://doi.org/10.1038/10.4254/wjh.v17.i2.100033>

- [3] Hu N, Yan G, Tang M, Wu Y, Song F, Xia X, Chan LW, Lei P (2023) CT-based methods for assessment of metabolic dysfunction associated with fatty liver disease. *European Radiology Experimental* 7(1):72. <https://doi.org/10.1038/10.4254/10.1186/s41747-023-00387-0>
- [4] Chupetlovska K, Akinci D'Antonoli T, Bodalal Z, et al (2025) ESR Essentials: a step-by-step guide of segmentation for radiologists - practice recommendations by the European Society of Medical Imaging Informatics. *European Radiology*. <https://doi.org/10.1007/s00330-025-11621-1>
- [5] Ying H, Liu X, Zhang M, et al (2024) A multicenter clinical AI system study for detection and diagnosis of focal liver lesions. *Nature Communications* 15(1):1131. <https://doi.org/10.1038/s41467-024-45325-9>
- [6] He X, Li Y, Zhao D, et al (2024) MSAT: biologically inspired multistage adaptive threshold for conversion of spiking neural networks. *Neural Comput & Applic* 36:8531–8547. <https://doi.org/10.1007/s00521-024-09529-w>
- [7] Xue X, Wimmer RD, Halassa MM, et al. (2023) Spiking Recurrent Neural Networks Represent Task-Relevant Neural Sequences in Rule-Dependent Computation. *Cogn Comput* 15, 1167–1189. <https://doi.org/10.1007/s12559-022-09994-2>
- [8] Yang Y, Ren J, Duan F (2023) The Spiking Rates Inspired Encoder and Decoder for Spiking Neural Networks: An Illustration of Hand Gesture Recognition. *Cogn Comput* 15, 1257–1272. <https://doi.org/10.1007/s12559-022-10027-1>
- [9] Rudnicka Z, Szczepanski J, Pregowska A (2025) Integrating Complexity and Biological Realism: High-Performance Spiking Neural Networks for Breast Cancer Detection, arXiv:2506.06265.
- [10] Doborjeh M, Doborjeh Z, Merkin A. et al. (2022) Personalized Spiking Neural Network Models of Clinical and Environmental Factors to Predict Stroke. *Cogn Comput* 14, 2187–2202. <https://doi.org/10.1007/s12559-021-09975-x>
- [11] Patankar M, Chaurasia V, Shandilya M (2025) A novel spiking neural network method for classification of tuberculosis using X-ray images. *Computers and Electrical Engineering* 122:110003. <https://doi.org/10.1016/j.compeleceng.2024.110003>
- [12] Gilani SQ, Syed T, Umair M, Marques O (2023) Skin cancer classification using deep spiking neural network. *Journal of Digital Imaging* 36(3),1137–1147. <https://doi.org/10.1007/s10278-023-00776-2>
- [13] Heidarian M, Karimi G, Payandeh M (2024) Effective multispike learning in a spiking neural network with a new temporal feedback backpropagation for breast cancer detection. *Expert Systems with Applications* 252(15),PartB:124010. <https://doi.org/10.1016/j.eswa.2024.124010>
- [14] Dehariya A, Shukla P (2021) Medical diagnosis model based on spiking neural network considering normalization of histogram and wavelet transform features of medical images. *International Journal of Engineering Trends and Technology* 69(7):159–166. <https://doi.org/10.14445/22315381/IJETT-V69I7P222>
- [15] Indiveri G, Chicca E, Douglas RJ (2009) Artificial Cognitive Systems: From VLSI Networks of Spiking Neurons to Neuromorphic Cognition. *Cogn Comput* 1, 119–127. <https://doi.org/10.1007/s12559-008-9003-6>
- [16] Rudnicka Z, Szczepanski J, Pregowska A (2024) Artificial Intelligence-Based Algorithms in Medical Image Scan Segmentation and Intelligent Visual Content Generation-A Concise Overview. *Electronics* 13(4):1–35. <https://doi.org/10.3390/electronics13040746>
- [17] Wu D, Jin G, Yu H, Yi X, Huang X (2025) Optimizing event-driven spiking neural network with regularization and cutoff. *Frontiers in Neuroscience* 19:1522788. <https://doi.org/10.3389/fnins.2025.1522788>
- [18] Dong JF, Jiang RH, Xiao R, Yan R, Tang HJ (2022) Event stream learning using spatio-temporal event surface. *Neural Networks* 154:543–559. <https://doi.org/10.1016/j.neunet.2022.07.010>
- [19] Zhan Q, Liu G, Xie X, Zhang M, Sun G (2023) Bio-inspired active learning method in spiking neural network. *Knowledge-Based Systems* 261:110193. <https://doi.org/10.1016/j.knosys.2022.110193>
- [20] Zenke F, Vogels TP (2021) The remarkable robustness of surrogate gradient learning for instilling complex function in spiking neural networks. *Neural Computation* 33(4):899–925. https://doi.org/10.1162/neco_a_01367
- [21] Antonelli M, Reinke A, Bakas S, et al (2022) The Medical Segmentation Decathlon. *Nature Communications* 13:4128. <https://doi.org/10.1038/s41467-022-30695-9>
- [22] Dong X, Tan Q, Xu S, Zhang J, Zhou M (2025) Ultrasound image-based contrastive fusion non-invasive liver fibrosis staging algorithm. *Abdominal Radiology*. <https://doi.org/10.1007/s00261-025-04991-z>
- [23] Javanshir A, Nguyen TT, Mahmud MAP, Kouzani AZ (2023) Training Spiking Neural Networks with Metaheuristic Algorithms. *Appl. Sci.* 13:4809. <https://doi.org/10.3390/app13084809>

- [24] Lonning K, Caan MWA, Nowee ME, Sonke JJ (2024) Dynamic recurrent inference machines for accelerated MRI-guided radiotherapy of the liver. *Computerized Medical Imaging and Graphics* 113:102348. <https://doi.org/10.1016/j.compmedimag.2024.102348>
- [25] Ying H, Liu X, Zhang M, Ren Y, Zhen S, Wang X, Liu B, Hu P, Duan L, Cai M, Jiang M, Cheng X, Gong X, Jiang H, Jiang J, Zheng J, Zhu K, Zhou W, Lu B, Zhou H, Shen Y, Du J, Ying M, Hong Q, Mo J, Li J, Ye G, Zhang S, Hu H, Sun J, Liu H, Li Y, Xu X, Bai H, Wang S, Cheng X, Xu X, Jiao L, Yu R, Lau WY, Yu Y, Cai X. (2024) A multicenter clinical AI system study for detection and diagnosis of focal liver lesions. *Nat Commun.* 15(1):1131. <https://doi.org/10.1038/s41467-024-45325-9>
- [26] Yasaka K, Akai H, Kunimatsu A, Abe O, Kiryu S. (2018) Liver Fibrosis: Deep Convolutional Neural Network for Staging by Using Gadoteric Acid-enhanced Hepatobiliary Phase MR Images. *Radiology* 287(1):146–155. <https://doi.org/10.1148/radiol.2017171928>
- [27] Choi KJ, Jang JK, Lee SS, Sung YS, Shim WH, Kim HS, Yun J, Choi JY, Lee Y, Kang BK, Kim JH, Kim SY, Yu ES. (2018) Development and Validation of a Deep Learning System for Staging Liver Fibrosis by Using Contrast Agent-enhanced CT Images in the Liver. *Radiology* 289(3):688–697. <https://doi.org/10.1148/radiol.2018180763>
- [28] Yin Y, Yakar D, Dierckx RAJO. et al. (2021) Liver fibrosis staging by deep learning: a visual-based explanation of diagnostic decisions of the model. *Eur Radiol* 31:9620–9627. <https://doi.org/10.1007/s00330-021-08046-x>